International Journal of Robotics and Automation, Vol. 36, 2021

Special Issue: Automatic Detection and Assessment of Bridge Structures

EXPERIMENTAL RESEARCH ON ULTIMATE BEARING CAPACITY OF A COMPOSITE ARCH RING CONSIDERING SECONDARY STRESS

Junxin Wang,* Weicheng Wang,* Feixiong Yang,** and Lei Chen***

Abstract

In this study, experimental research on the ultimate bearing capacity of a reinforced concrete composite arch ring was carried out. Considering the influence of the initial stress, the thickness of the reinforcement layer, the eccentricity of the load before reinforcement, the material performance, bearing capacity, failure mode, and load-strain relationship were analysed. The test results showed that the bearing capacity of the reinforced structure decreased with the increase of the initial stress, but there was not a proportional relationship between them. They were affected by the synergistic force and material nonlinearity between the old and the new structures. When the reinforced layer was located on the side of the smaller compression, the increase of the thickness of the reinforced layer contributed to the ultimate bearing capacity of the structure. Moreover, the increase of the eccentricity made the bearing capacity of the reinforced structure decrease rapidly. In addition, bar planting and chipping before reinforcement could effectively enhance the integrity of the composite section. Therefore, it could be considered that the deformation of the composite section after reinforcement met the assumption of a flat section.

Key Words

Masonry arch bridge, bearing capacity, initial stress, secondary stress, composite arch ring

1. Introduction

By the end of 2017, the number of permanent bridges in China exceeded 1 million, ranking first in the world. With the continuous development of China's transportation industry, the problems of overloading, overweight, and the environment are serious. Coupled with the natural ageing of the bridges themselves, the number of old dangerous bridges is gradually increasing, including nearly 100,000 dangerous bridges across the country. In recent years, the number of dangerous bridges in China has increased. In the southwestern part of China, masonry arch bridges have been widely used due to their advantages of convenient raw materials, low cost, and potential bearing capacity [1]. According to the statistics of the Highway Bureau (at the end of 2009), among the 1,713 bridges surveyed by various districts and counties in Chongqing, completed arch bridges accounted for the vast majority, with 1,533 arch bridges accounting for 89.5% of the total bridges.

Masonry arch bridges have made great contributions to the construction of highways in China, but most of the in-service masonry arch bridges were built in the 1960s and 1990s, with low design loads during construction. Due to the long-term use, environmental pollution, and other natural factors [2], [3], the bridges have gradually become old bridges so that they cannot meet normal operational requirements [4], [5], and bridge collapse accidents can even occur. Faced with numerous old dangerous bridges, the demolition and reconstruction have been not only a huge investment but also a higher "comprehensive" cost paid by the entire society during the new construction period. In response to the previous requirements, in the long-term engineering practice, various reinforcement techniques for improving the bearing capacity and mechanical performance of arch bridges have emerged. The reinforcement research about the masonry arch bridges has become an important topic in the field of bridges [6], [7]. At present, for the superstructure of a solid belly arch bridge, the widely used reinforcement methods around the world are the reinforced concrete composite arch ring reinforcement method, the fixed arch on-load method, the multi-point support system reinforcement method, the paste reinforcement method, and the system conversion method [8]–[12].

* School of Civil Engineering, Chongqing Jiaotong University, Chongqing, China; e-mail: meteorpretty@126.com, JTwcwang@163.com

** Sichuan Yakang Expressway Co., Ltd, Ya'an, China; e-mail: FeiX_Yang@163.com

*** Chongqing Municipal Design Institute, Chongqing, China; e-mail: 526512986@qq.com

Corresponding author: Weicheng Wang

Recommended by Dr. Jingzhou Xin

(DOI: 10.2316/J.2021.206-0537)

The reinforced concrete composite arch ring reinforcement method [13], [14] is one of the most common methods for solid belly arch bridge reinforcement. Before the arch bridge is strengthened, the original arch ring has already been loaded. The weight of the newly added reinforcement layer after the reinforcement is assumed by the original structure, while the post-loading loads are assumed by the newly added part [15], [16]. Therefore, the reinforcement structure has the characteristics of a multi-stage load that is the secondary force, making a large difference between the new and old arch rings. The original arch ring has been subjected to a certain load before reinforcement. Therefore, the strain generated in the newly added arch ring has been delayed during the process of the new and old structures cooperating with the new load [17], [18].

Zhang and Qian [19] analysed the ultimate state of a reinforced composite section, and they obtained three forms of boundary damage according to the possible strain distribution. Huang *et al.* [20] considered that a composite section conformed to the assumption of flat section, and they deduced the conclusion that the bending moment would be distributed according to the stiffness of the new and old sections. However, the influence of the initial stress of the original arch ring was not taken into account, and the non-linearity of the material before and after reinforcement could not be accounted for simultaneously after the conversion of the section. Sun *et al.* [21] proposed a finite element method for calculating the ultimate bearing capacity of composite arch rings by combining the separated model with the integral continuous model, and they analysed the ultimate bearing capacity of composite arch rings for various reinforcement parameters. Zhu *et al.* [22] put forward the idea that the bearing capacity range of a composite section under secondary loading was deduced when the allowable strain at each point of the strain slope section was known. Therefore, the idea was of great reference significance for the calculation of the bearing capacity of a composite section strengthened by a composite arch ring.

Although the composite arch reinforcement method has been used for a long time in the reconstruction of masonry arch bridges, its corresponding theoretical research area is still small and needs to be strengthened. There are many influencing factors on the bond performance and bearing capacity of a new and old arch ring interface under the secondary stress. To improve the ultimate bearing capacity of a reinforced arch bridge, various influence parameters of the initial stress, the thickness of reinforcement layer, and the loading eccentricity were studied in this research.

2. Reinforcement Mechanism of a Composite Arch Ring

The reinforcement technology of the reinforced concrete composite arch ring was an effective method for the main arch ring due to the deformation of the arch axis and the cracking of the main arch ring, which caused the insufficient bearing capacity or functional failure of the whole structure. After reinforcement, the composite arch ring had a greater increase in rigidity and strength than the original arch ring, which could significantly improve the bearing capacity of the arch bridge and extend the service life of the structure [23]–[25]. The reinforcement mechanism of the reinforcement technology could be started with the following points.

2.1 Mechanism of the Increasing Section

Using the bonding force of the anchor rod and the cast-in-place concrete itself, the cast-in-place reinforced concrete reinforcement layer and the original main arch ring structure layer were organically bonded together, thereby effectively increasing the sectional area. The structural compressive rigidity and the bending resistance were greatly improved after the reinforcement so that the burden of the original structure was effectively shared.

2.2 Closure Mechanism of the Cracks

After the reinforcement, because of the reinforced concrete reinforcement layer, the surface crack of the original main arch ring became an internal crack, and the stress intensity factor was greatly reduced, which was very advantageous for suppressing the crack propagation. This also showed that even if the original structure had cracks at the edge stress of the section before the reinforcement reached (or exceeded) the allowable stress, the structure could still be strengthened to reduce the stress intensity factor and prevent the crack from continuing to develop. The structure could continue to be carried after reinforcement.

2.3 Centralized Closing Force Cracking Mechanism of the Crack Tip

The stress intensity factor superposition method (K superposition method) was based on the principle of linear elastic fracture mechanics. The effect of the reinforced concrete reinforcement layer of the main arch ring was equivalent to the application of a pair of concentrated closing forces at the crack tip (the crack initiation point). Moreover, the negative stress intensity factor that was generated by the closing force could prevent the crack from developing (Fig. 1). When the crack on the main arch ring was about to expand, the reinforcing layer of the reinforced concrete composite main arch ring would inevitably produce a strong concentration force for suppressing crack development, greatly reducing the stress intensity factor at the crack and actively suppressing the crack initiation.

2.4 Integral Mechanism of the Reinforcing Arch Ring with Cracks

The reinforced concrete composite main arch ring technology was used to anchor the original arch ring to the newly poured concrete arch plate under the action of the anchor rod. This improved the integrity of the original arch ring structure and made the original arch ring with a crack work in a united fashion. It also improved the stress condition of the arch ring section and exerted the strength of the material more fully.

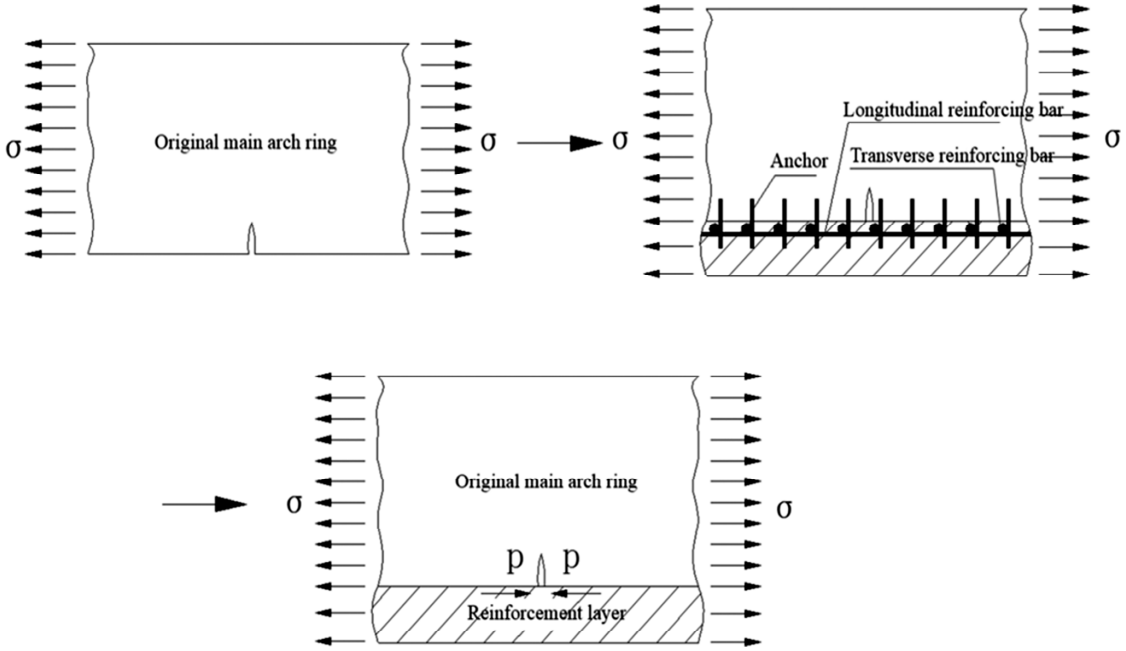

Figure 1. Schematic of the crack resistance of the reinforcement layer.

Table 1
Parameter Design of Specimens

Label	Pre-Reinforcement Section (mm)	Original Structural/ Reinforcement Layer Materials	Reinforcement Layer Thickness (mm)	Reinforced Protective Layer Thickness (mm)	Initial Stress Ratio	Loading Eccentricity (mm)
A	200×140	C30/None	–	–	0	0
B	200×140	C30/None	–	–	0	−30
C	200×140	C30/C50	70	35	0	−30
D	200×140	C30/C50	70	35	0.15	−30
E	200×140	C30/C50	70	35	0.15	+30
F	200×140	C30/C50	70	35	0.3	−30
G	200×140	C30/C50	70	35	0.3	−60
H	200×140	C30/C50	35	17.5	0	−30
I	200×140	C30/C50	35	17.5	0.15	−30

3. Test Scheme

3.1 Specimen Design

In this test, the original structure of the masonry arch bridge was simulated with a C30 plain concrete column. The masonry arch bridge had good compressive performance work, so the design of the component was mainly based on the small eccentric compression. In this case, the effect of the reinforcing layer reinforcement was small. Therefore, a detailed study on the reinforcement ratio of the reinforcing layer steel bars was not carried out. The influences of the initial stress, the thickness of the reinforcement layer, and the loading eccentricity on the bearing capacity of the structure were considered. In total, nine specimens were designed, including two unreinforced columns and seven reinforced columns. The specific specimen size and parameters settings can be seen in Table 1. In addition, the initial stress was expressed by the stress level β, which was the axial force load of the initial stress axial load relative to the same loading that the structure could withstand. To avoid the influence of the slenderness ratio and the additional eccentricity, the design of the specimen met the requirement of a slenderness ratio smaller than 8. The cross section of the column was 200 mm × 140 mm and the height was 800 mm. To prevent local crushing that would affect the final bearing capacity value, a reinforced concrete cushion with a thickness of 200

Figure 2. Test specimen and a pre-stressed tensioning device.

cm was provided at both ends. Three layers of steel mesh were arranged in the cushion layer, and the steel plate was partially placed during the test loading.

For the reinforcement specimens, to facilitate the pouring reinforcement layer, the pre-stressed tension anchoring, and the local compression damage, the pad beams with thicknesses of 100 cm were arranged on the upper and lower parts of the specimens before the reinforcement. The goals were to seal the pre-stressed anchoring section, protect the pre-stress, enhance the local performance, and maintain the same level of height as the unreinforced column.

For the specimen that needed to simulate the initial stress, the PVC pipe was reserved for later tensioning. Sprinkle water conservation was used after pouring, and natural conservation was used after 4 days. After 1 month of component maintenance, pre-stressed tension was applied. The pre-stressed tendons were in the form of single-end tension, and the test specimens and pre-stressed tensioning devices were as shown in Fig. 2.

3.2 Reinforcement Scheme

The reinforced concrete reinforcement layer was applied to the completed structure about 7 days after the completion of the pre-stressed tensioning. The reinforcement layer was made of C50 concrete and the steel bars are made of HRB400. First, the reinforcement surface of the work column was drilled and cleaned, and the reinforcement layer was tied and planted. The implanted steel bar was Φ8, and the longitudinal steel bar was Φ12. Then, after injecting glue into the implant hole, the steel bar was rotated and implanted. Finally, after the gel was solidified for 48 h, the reinforcement layer was longitudinally stressed.

Before pouring the concrete of the reinforcement layer, the cross-section steel bar was polished, the steel strain gauge was pasted, and the silicone protective layer was applied, as shown in Fig. 3. As the reinforcement layer was closer to the interface joint, it was necessary to pay attention to the timely vibration during concrete pouring so that the concrete could be poured properly. The mould was demolished after 3 days and cured according to the specification that the age should be over 28 days.

Figure 3. Reinforced layer steel strain gauge paste.

3.3 Loading Scheme

In this test, the components were loaded under static load, and the test was carried out under a 1,000-kN press. Before the formal test of each specimen, preloading was required to eliminate the inelastic deformation error caused by the uneven contact of equipment and spacers. The specimens were loaded at a constant rate during formal loading until the structure was broken. To avoid the partial compression of the components, in addition to the steel mesh placed at both ends of the component, a steel backing plate was provided at the end of the loading. The eccentric compression and the control of the height of the compression zone could be achieved by adjusting the position of the steel backing plate, as shown in Fig. 4.

The data to be tested in this test was as follows: (1) the failure load value of the specimen, (2) the initiation process of the crack and the failure mode, (3) the strain value of the longitudinal reinforcement, and (4) the strain value of the characteristic section of the original structure and the reinforcement layer concrete. For each specimen, the surface of the reinforcement layer and the concrete structure were attached with a strain gauge, the data for which was collected and recorded by the corresponding change of the crystal grain resistance strain gauge. The layout diagram of the section strain gauge is shown in Fig. 5. To avoid the danger caused by the collapse of the specimen during the loading process, the whole process of the test was recorded to supplement the phenomenon that

was not observed in time during the loading. The position and development form of the crack were analysed, and the corresponding bearing capacity value was recorded.

The loading position of each group of specimens is shown in Fig. 6. The combined section-shaped mandrel was obtained according to the elastic mode conversion.

Figure 4. Load device and settings of the local pad.

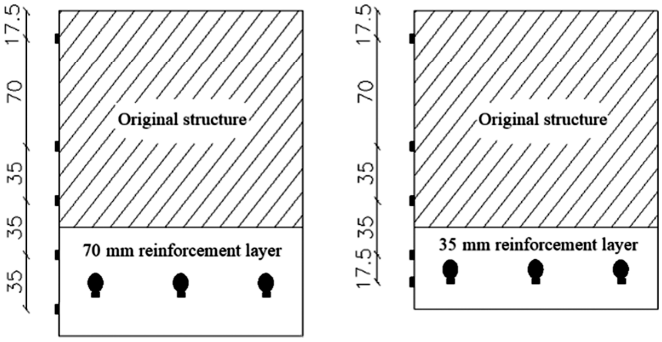

Figure 5. Column strain gauge measurement point layout.

The eccentricity was negative near the original section side and positive near the reinforcement side. A and B were unreinforced specimens: A was the axial compression, and B was the eccentric compression with an eccentricity of −30 mm. C, D, E, F, and G were specimens with a thickness of 70 mm. The specimens C, D, and F had initial stresses of 0, 0.15, and 0.3, respectively, and they were eccentric compression specimens with an eccentricity of −30 mm. The initial stress of specimen E was 0.15, and the eccentricity was +30 mm. The initial stress of specimen G was 0.3, and the eccentricity was −60 mm; H and I were specimens with a reinforcement layer of 35 mm; the initial stresses were 0 and 0.15, respectively, and the eccentric distance was −30 mm.

4. Test Analysis and Results

4.1 Material Performance Analysis

4.1.1 Concrete Mechanics Parameter Test

When pouring the original structure and the reinforcement layer, six or more standard pieces of 150 mm × 150 mm × 150 mm and 150 mm × 150 mm × 300 mm standard prism specimens were prepared for the compressive strength test, as shown in Fig. 7.

4.1.2 Steel Mechanical Parameters Test

The strength of the steel cushion, the embedded steel bars, and the reinforcement of the longitudinal steel bars were all measured according to the actual measurement. For each of the three different samples, the metal tensile test was carried out according to the specifications, as shown in Fig. 8.

After the standard test of the material, the design value of the C30 concrete cube compressive strength was

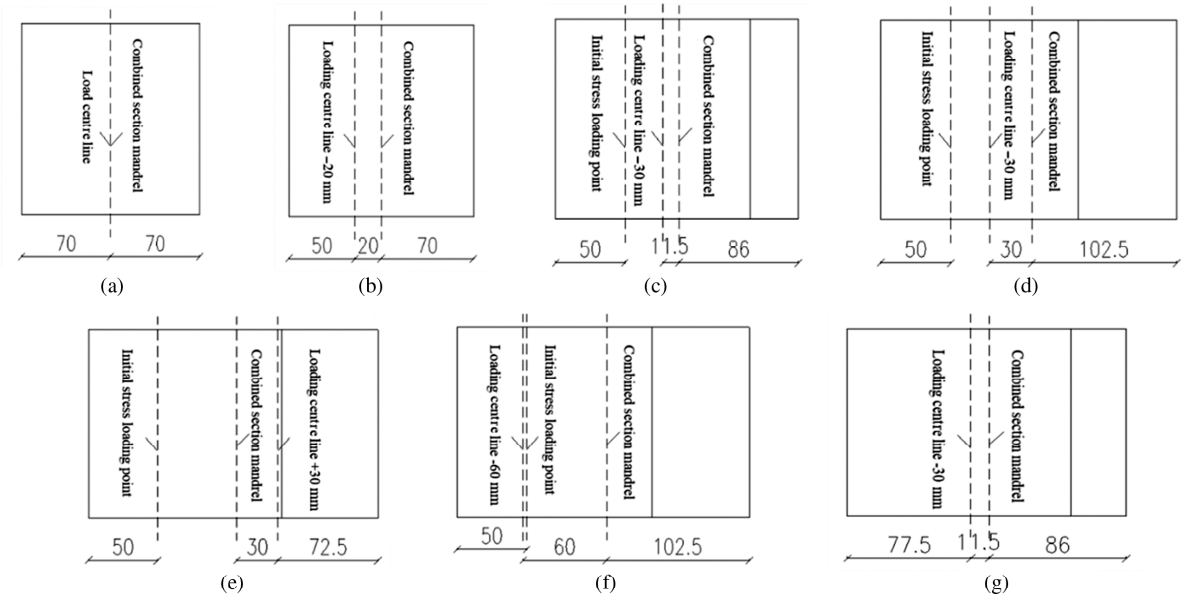

Figure 6. Loading position diagram: (a) specimen A; (b) specimen B; (c) specimen I; (d) specimen C, D, and F; (e) specimen E; (f) specimen G; and (g) specimen H.

Figure 7. Destruction picture of the standard cubes and standard prisms.

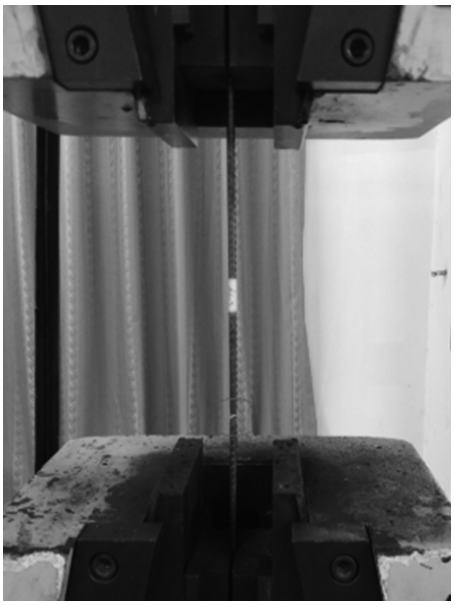

Figure 8. Steel bar drawing test.

32.5 MPa, the design value of the C50 concrete cube compressive strength was 48.0 MPa, and the yield strength of the HRB400 steel was 411.2 MPa.

4.2 Bearing Capacity Analysis

The ultimate bearing capacity of each specimen is shown in Table 2. The test data showed that specimen E had the maximum bearing capacity. Its reinforcement thickness was 70 mm, the tensile stress was 190 kN, and the eccentricity was 30 mm near the reinforcement side.

It can be seen from Fig. 9(a) that when the specimen was not reinforced, the eccentrically compressed specimen B had a 20% lower bearing capacity than the axially compressed specimen A. A similar trend can be observed in Fig. 9(c). At the same initial stress level, the eccentric specimen G had a 31% lower bearing capacity than the axial specimen F. As shown in Fig. 9(d), for the same eccentricity, the bearing capacity of the specimens with different eccentric directions differed greatly. Therefore, it could be concluded that similar to the unreinforced specimens, the bearing capacity of the reinforced components decreased rapidly with the increase of the eccentricity. However, the difference between the initial stress of the original structure and the eccentric direction of the secondary force was different. There were differences in the trend of the bearing capacity.

Table 2
Ultimate Bearing Capacity When the Specimen Was Damaged

Specimen	Reinforcement Layer Thickness (mm)	Eccentric Position (mm)	Ultimate Bearing Capacity (kN)
A	0	0	851.04
B	0	−20	682.765
C	70	−30	1,112.468
D	70	−30	1,002.655
E	70	30	1,694.2
F	70	−30	790.24
G	70	−60	544.82
H	35	−30	1,030
I	35	−30	744

It can be seen from Fig. 9(b) that for the same eccentric loading condition, the structural bearing capacity decreased with the increase of the initial stress. The relative stress decreased by 9.9% when the initial stress was 0.15 and the relative decrease was 29% when the initial stress was 0.3. The decrease of the bearing capacity was not proportional to the increase of the initial stress.

It can be seen from Fig. 9(e) that the bearing capacity of the structure after reinforcement was obviously improved. Compared with the thickness of 35 mm, however, the bearing capacity was only increased by about 8% when the thickness of the reinforcing layer was 70 mm. Therefore, under the force of the test, the bearing capacity did not improve much when the thickness of the reinforcing layer was increased to a certain extent. Therefore, it was not necessary to use an excessively large reinforcing layer thickness.

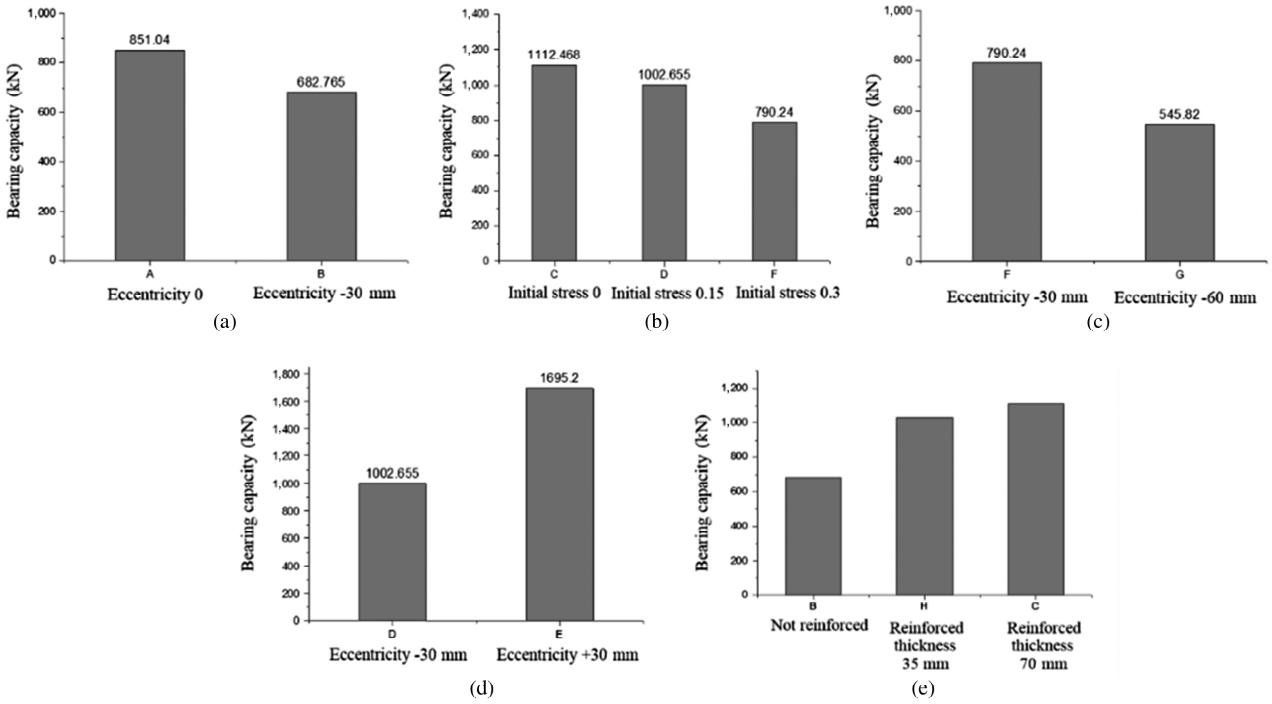

Figure 9. Comparison of the ultimate bearing capacity: (a) different eccentricities before reinforcement; (b) different initial stresses; (c) different eccentricities; (d) eccentricity in different directions; and (e) different reinforcement layer thicknesses.

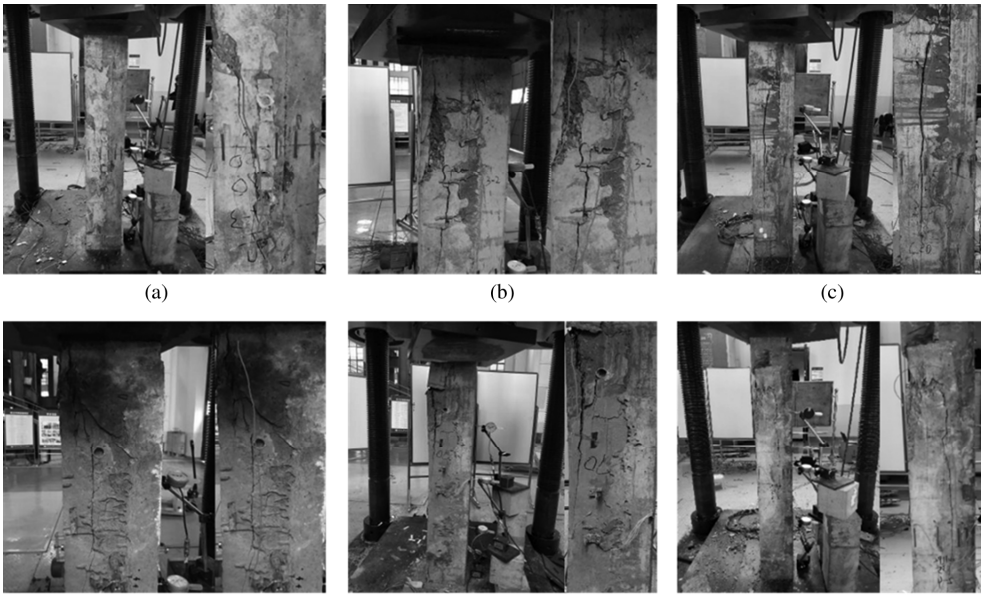

Figure 10. Photographs of the failure modes of different concrete column specimens: (a) specimen C; (b) specimen D; (c) specimen E; (d) specimen F; (e) specimen G; and (f) specimen H.

4.3 Failure Morphology Analysis

The damage pattern photographs of the respective specimens were summarized, as shown in Fig. 10.

4.3.1 Unreinforced Specimen

For the unreinforced specimens A and B, the failure modes were brittle fracture under the action of the axial and eccentric compression loads. When the load was applied to 60%–75% of the ultimate load, the concrete core crack occurred near the middle section of the column, and the crack increased with the concrete spalling, causing the pressure area to decrease rapidly. Finally, the component broke down and collapsed. The eccentric compression specimen B had a similar failure mode, the destruction speed was fast, and the damage photograph was not obtained in time.

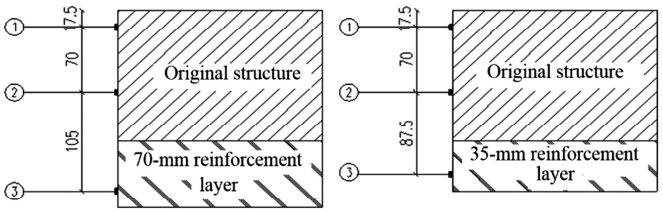

Figure 11. Measuring point layout of the specimen cross-section strain.

4.3.2 Specimens with a Reinforcement Layer Thickness of 70 mm

For specimen C, the reinforcement layer was located on the smaller pressure side, and the original structure was located on the larger pressure side. When the adjacent structure was close to the axial force side, the concrete first reached the ultimate compressive strain, and it was partially crushed and cracked. Then the cracking development was faster, and it was accompanied by some concrete spalling. Finally, the specimen quickly reached the ultimate bearing capacity, such as small eccentric damage.

For specimen E, the reinforcement layer was located on the side where the pressure was large, and the original structure was close to the axial force side when the failure occurred. In other words, the side close to the reinforcement layer first reached the ultimate strain. Then the concrete was locally crushed and accompanied by crack development, and then the structure was rapidly destroyed. The reinforcement layer remained intact when destroyed.

The forces of specimens F and D were similar to that of C. The reinforcement layer was located on the tension side. The initial stresses of D and F were 0.15 and 0.3, respectively. When both specimens were destroyed, the original structure was close to the axial force and the ultimate compressive strain was reached. The difference was that D had a relatively small initial crushing area and a larger crushing area than F, indicating that the internal force distribution was more uniform, and thus, had a larger ultimate bearing capacity.

Specimen G was similar to specimen F, but the eccentricity was larger than that of F. Therefore, the local crushing area was small when broken, and the local crushing area was partially broken when the cross section was not fully utilized, resulting in a low bearing capacity.

4.3.3 Specimens with a Reinforcement Layer Thickness of 35 mm

Specimen H was similar to specimen I. The thickness of the reinforcement layer was 35 mm, and both specimens were located on the side with less pressure. The initial stresses were 0 and 0.15, respectively. When the failure occurred, the original structure was crushed near the edge of the axial force. The difference was that the failure of specimen I was due to the existence of initial stress. The crushing area was relatively small, and the bearing capacity was relatively low.

4.4 Analysis of the Load–Strain Relationship

The concrete strain value was recorded during the loading process. For the convenience of analysis, only part of the strain data was extracted, such as the strain at the middle section of the column at ①–③. The position of the specific strain point is shown in Fig. 11.

To quantitatively analyse the load-strain relationship of the specimen, the statistical load values were 0.1, 0.3, 0.5, 0.7, and 0.9 (the ultimate load of each specimen at the time of failure). The strain values of the reinforced specimens were drawn. The line chart is shown in Fig. 12.

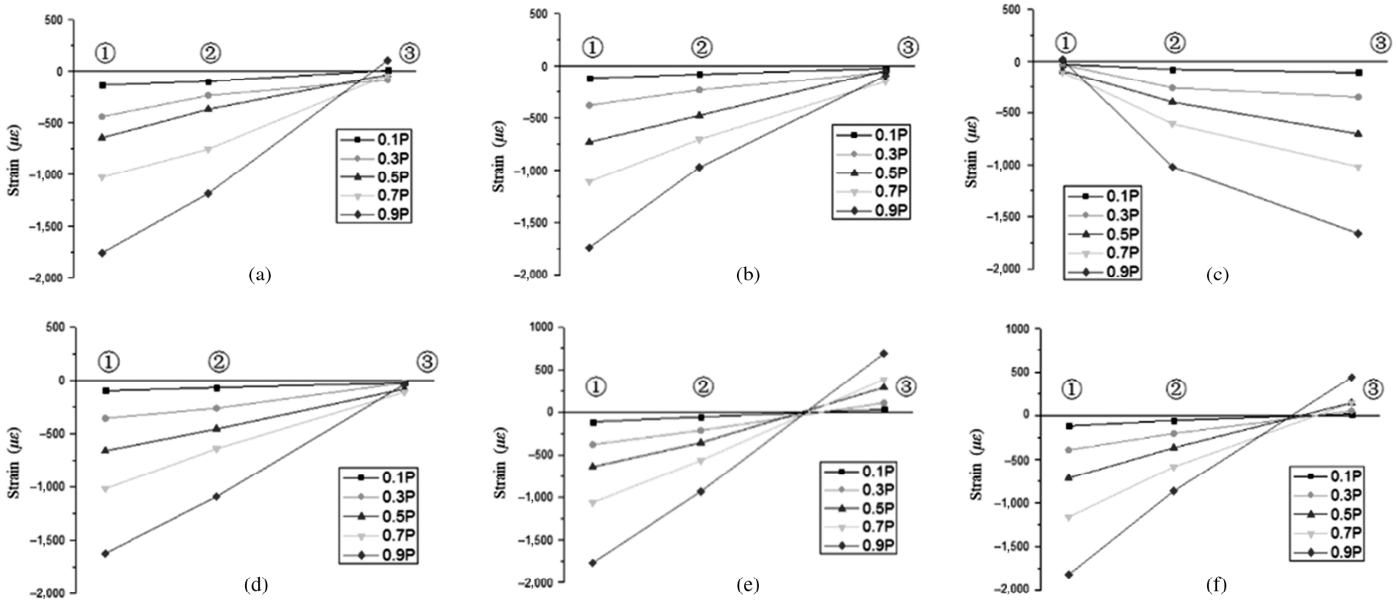

Figure 12. Strain profiles of the cross sections of the specimens: (a) specimen C; (b) specimen D; (c) specimen E; (d) specimen F; (e) specimen G; and (f) specimen H.

Table 3
Steel Strain Value of Each Specimen under the Ultimate Load

Specimen Label	C	D	E	F	G	H	I
$\varepsilon_s(\mu\varepsilon)$	64	72	2,787	−152	−804	−471	−444

The test data showed that in the initial stage of loading, the deformation of the new and old concrete conformed to the flat section assumption. As the load increased by more than 0.7, the new and old concrete layers gradually no longer had coordinated deformation, but they were closer to the straight-line segment until 0.9. At the same time, from the failure mode of the specimen, the old and new concrete layers were still effectively connected until the structure was destroyed. Therefore, we could assume that the deformation of the composite section essentially satisfied the flat section assumption until the composite section was destroyed.

Due to the small eccentricity of the test, the steel bar in the reinforcement layer did not yield. The strain values of the reinforcement in the tension zone are shown in Table 3.

5. Conclusion

In this research, the bearing capacity test of a composite arch ring was carried out. The test specimen design, reinforcement scheme, and loading scheme were introduced. The material properties, bearing capacity, failure mode, and load-strain relationship were analysed. The conclusions were as follows:

1. Combined with the reinforcement of a reinforced concrete composite arch ring, the purpose and the content of the test were clarified. Considering the influence of the initial stress of the structure, the thickness of the reinforcement layer, and the load eccentricity on the bearing capacity of the structure, the static test loading scheme was determined. Additionally, the data and the collection points required for the test were clarified.
2. With the increase of initial stress, the bearing capacity of the structure was reduced after the reinforcement. However, due to the interaction of the new and old structures and the nonlinearity of the material, the increase of the initial stress was not proportional to the decrease of the structural bearing capacity. When the pressure was on the smaller side, the increase of the thickness of the reinforcement layer did not contribute much to the ultimate bearing capacity of the structure. Similar to the structural stress before the reinforcement, the increase of the eccentricity would also cause the bearing capacity of the reinforcement structure to decrease rapidly. If the eccentricity of the structure was reduced or the reinforcement layer was located on the side with a large pressure, the ultimate bearing capacity of the structure would be greatly improved.
3. After the section strain data that were collected during the loading process was sorted, it was found that the composite section had a coordinated deformation and good joint force performance. When loaded to 90% of the ultimate load, the strain distribution of the section was also approximately linear, which was consistent with the flat section assumption. In addition, from the failure mode of the specimen, the new and old concrete layers were still effectively and closely bonded together. It was indicated that the reinforcement and the chisel could effectively enhance the integrity of the composite section before reinforcement. Therefore, it could be considered that the deformation of the composite section satisfied the flat section assumption after reinforcement.

Acknowledgement

This research was financially supported by Science and Technology Project of Guizhou Provincial Transportation Department (2018-123-001), Science and Technology Project of Hubei Provincial Transportation Department (2020-2-1-1).

References

[1] B.C. Chen, View and review of arch bridge technology, *Journal of Fuzhou University (Natural Science Edition)*, *37*(1), 2009, 94–106.

[2] F.Q. Guo and Z.W. Yu, Influencing factors of ultimate bearing capacity of in-service long span stone arch bridge, *Journal of Railway Science and Engineering*, *9*(2), 2012, 14–17.

[3] X.W. Li and X. Yuan, Analysis of deterioration mechanism and research of comprehensive strengthening techniques for solid spandrel circular arch bridges, *World Bridges*, *4*, 2007, 66–69.

[4] L.L. Zhang, S.M. Liu, L.Q. Wu, and J.T. Zhou, The safety assessment model of stone arch bridge based on fuzzy synthetic evaluation, *Journal of Civil, Architectural & Environmental Engineering*, *33*(S1), 2011, 194–198.

[5] S.M. Liu and L.Y. Zhang, Optimizing method for strengthening and loading program of masonry arch bridge, *Bridge Construction*, *43*(6), 2013, 88–93.

[6] Q.F. Deng, The study on concrete bridge strengthening and reconstruction technology, *Shanxi Science & Technology of Communications*, *2*, 2006, 43–45.

[7] B.H. Liao and G.D. Wang, Research and application of new methods for arch bridge reinforcement, *Highway*, *10*, 2006, 34–37.

[8] L.C. Zhou, Y.F. Zheng, and F.M. Liu, Research on reinforcement technology of upper structure of stone arch bridge, *Railway Engineering*, *8*, 2010, 36–38.

[9] L. Garmendia, J.T. San-José, D. García, and P. Larrinaga, Rehabilitation of masonry arches with compatible advanced composite material, *Construction and Building Materials*, *25*(12), 2011, 4374–4385.

[10] Y. Zhou, Discussion on reinforcement design and construction method of stone arch bridge, *Shanxi Architecture*, *41*(2), 2015, 155–156.

[11] L.J. Liu, Y. Qin, Y. Zhang, and H.Z. Gao, Effects of re-force on steel-strengthened reinforced beam's capacity, *Journal of Chang'an University (Natural Science Edition)*, *31*(1), 2011, 46–50.

[12] Z.W. Yu, Reinforcement method of in-service stone arch bridge with steel-concrete composite structure, *Journal of Railway Science and Engineering*, *9*(1), 2012, 1–4.

[13] S.H. Chen, M.Y. Yang, and H.Y. Pan, Application technology of hollow stone arch bridge reinforcement by composite main

arch, *Western China Communications Science & Technology*, *4*, 2015, 52–54.
[14] J.T. Zhou, Z.G. Li, and S.M. Liu, Reinforcement boundary of steel in the reinforcing layer of RC beam under the secondary Load, *Journal of Chongqing Jiaotong University (Natural Science)*, *34*(1), 2015, 30–33.
[15] Z.L. Wei, Q.H. Pu, and Z. Shi, Research on rational calculation model of solid-type stone arch bridge based on finite element analysis, *Railway Engineering*, *9*, 2010, 9–12.
[16] Y.Z. Wu, Discussion on reinforcement of stone arch bridge by wrapping main arch with reinforced concrete, *Road Machinery & Construction Mechanization*, *33*(8), 2016, 91–94.
[17] L. Garmendia, J.T. San-José, D. García, P. Larrinaga, and J. Díez, Innovative strengthening solution based on textile reinforced mortar for stone masonry arches, *Advanced Materials Research*, *133–134*, 2010, 849–854.
[18] Z.M. Zhao, F.J. Chen, J.Y. Chai, Z.J. Wang, and H.L. Zhou, Analysis and evaluation on strengthening and widening of a catenary stone arch bridge with solid spandrels, *Advanced Materials Research*, *838–841*, 2013, 1042–1047.
[19] J. Zhang and Y.J. Qian, Theoretical analysis of normal section bearing capacity of stone main arch ring strengthened by reinforced concrete, *Journal of Highway and Transportation Research and Development*, *25*(6), 2008, 76–80.
[20] H.D. Huang, Z.F. Xiang, J. Liu, and X.F. Lin, Study of internal force distribution method of co-section for arch bridges strengthening, *Journal of Chongqing Jiaotong University (Natural Science)*, *2*, 2008, 200–203.
[21] C. Sun, M. Liu, B.C. Chen, and Q.X. Wu, Research on ultimate load-carrying capacity of composite arch ring of stone arch bridge reinforced by concrete arch-lifted method, *Journal of Fuzhou University (Natural Science Edition)*, *40*(3), 2012, 376–382.
[22] C. Zhu, J.T. Zhou, S.M. Liu, and Z.G. Wu, Study on strain slope of co-section for bearing capacity of the strengthened masonry arch bridges, *Science Technology and Engineering*, *16*(10), 2016, 56–62.
[23] J.T. Zhou, Y. Hao, G.J. Liu, *et al.*, Reasonable reinforcement process and internal force analysis of stone arch bridge, *Highway*, *4*, 2005, 33–35.
[24] Q.Y. Liu, J.T. Zhou, L. Wang, and X.L. Zhu, Minimum thickness of reinforcing layer of stone arch bridge strengthened by section enlargement method, *Journal of Chongqing Jiaotong University (Natural Science)*, *27*(1), 2008, 20–23.
[25] C. Huang, S.M. Liu, and J.T. Zhou, Reinforcement effect evaluation of arch bridge based on co-section analysis method, *Journal of Chongqing Jiaotong University (Natural Science)*, *31*(3), 2012, 373–376.

Biographies

Junxin Wang was born in 1986. He received his master's degree in Civil Engineering in 2017, and now he is studying for a Ph.D. in Bridge and Tunnel Engineering at Chongqing Jiaotong University. His current research interests include bridge maintenance and temperature effect of concrete-filled steel tubular arch-bridge.

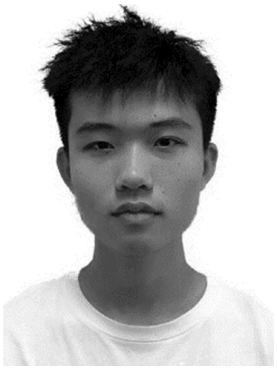

Weicheng Wang was born in 1996. He received his bachelor's degree in Road and Bridge in 2018. He is now studying for his master's degree in Architecture and Civil Engineering at Chongqing Jiaotong University. His current research interests include bridge engineering and ultra-high performance concrete.

Feixiong Yang was born in 1989. He is studying for his bachelor's degree in Engineering Management at Southwest Jiaotong University. He is now working in Sichuan Yakang Expressway Co., Ltd. His current research interest includes engineering management.

Lei Chen was born in 1994. He received his master's degree in Engineering in 2019. He is now working in Chongqing Municipal Design Institute. His current research interests include bridge detection and bridge reinforcement.